On Hybrid Model Predictive Control of Sewer Networks

Carlos Ocampo-Martinez[1], Alberto Bemporad[2], Ari Ingimundarson[1], and Vicenç Puig[1]

[1] Sistemes Avançats de Control, ESAII, Universitat Politècnica de Catalunya (UPC), Rbla. Sant Nebridi 10, Terrassa, 08222 Barcelona, Spain.
{carlos.ocampo,ari.ingimundarson,vicenc.puig}@upc.edu

[2] Department of Information Engineering, University of Siena, Via Roma 56, I-53100 Siena, Italy. bemporad@dii.unisi.it

Summary. *Real-Time Control* (RTC) of sewer network systems plays an important role in meeting increasingly restrictive environmental regulations to reduce release of untreated wastewater to the environment. This chapter presents the application of Hybrid Model Predictive Control (HMPC) on sewer systems. It is known from the literature that HMPC has a computational complexity growing exponentially with the size of the system to be controlled. However, the average solution time of modern *mixed integer program* (MIP) solvers is often much better than the predicted worst case solution time. The problem is to know when the worst case computational complexity appears. In addition to presenting the application, a secondary aim of the chapter is to discuss the limits of applicability due to real-time constraints on computation time when HMPC is applied on systems of large scale such as sewer systems. By using a case study of a portion of the Barcelona sewer system, it is demonstrated how the computational complexity of HMPC appears for certain state and disturbance combinations.

1 Background

1.1 Introduction

Real-Time Control of sewer network systems plays an important role in meeting increasingly restrictive environmental regulations to reduce release of untreated wastewater or *Combined Sewage Overflow* (CSO) to the environment. Reduction of CSO often requires major investments in infrastructure within city limits and thus any improvement in efficient use of existing infrastructure, for example by improved control, is of interest. The advantage of sewer network control has been demonstrated by a number of researchers the last decades, see [22, 34, 41, 42].

Extensive research has been carried out on real-time control of urban drainage systems. Comprehensive reviews that include a discussion of some existing implementations are given by [43] and cited references therein, while practical issues are discussed by [44], among others. The common idea is the use of optimization techniques to improve the system performance. Common control objectives are to try to avoid street flooding, prevent CSO discharges to the environment, minimize the pollution, uniform utilization of the sewer system storage capacity and, in most of cases, minimize the operating costs [21, 45, 46, 52]. The multivariable and

large scale nature of sewer networks has lead to the use of some variants of *Model Predictive Control* (MPC), as control strategies.

In order to apply MPC on a sewer system, a model able to predict its future states over a prediction horizon taking into account a rain forecast is needed. Sewer networks are systems with complex dynamics since water flows through sewers in open channel. Their dynamics are described by Saint-Vennant's partial differential equations that can be used to perform simulation studies but are highly complex to solve in real-time.

Several control oriented modeling techniques have been presented in the literature that deal with sewer systems, see [19, 34]. In [17, 39], a conceptual linear model based on assuming that a set of sewers in a catchment can be considered as a virtual tank or reservoir, has been used. The main reason to use a linear model is to preserve the convexity of the MPC optimization problem. A similar approach can be found in an early reference on MPC applied on sewer systems [22].

There exist however several inherent phenomena (overflows in sewers and tanks) and elements (weirs) in the system that result in distinct behavior depending on the state (flow/volume) of the network. These behaviors can not be neglected nor can they be modeled by a pure linear model. Instead, they require to be modeled using non-linear functions depending on logical conditions [34]. This leads to the use of modeling methodologies that allow the inclusion of both continuous and discrete dynamics. The continuous dynamic part is typically associated with physical first principles while the discrete dynamic part comes from logic conditions that establish commutations of operational mode depending on internal system variables. This mixture of logical conditions and continuous dynamics gives rise to a *hybrid system*.

1.2 Hybrid Systems and Mixed Logical Dynamical Systems

The hybrid systems considered in this chapter are *Mixed Logical Dynamical* (MLD) systems, introduced in [7]. MLD systems have recently been shown to be equivalent to other representations of hybrid systems such as *Linear Complementarity* (LC) systems, *Min-Max-Plus Scaling* (MMPS) systems and *Piecewise Affine* (PWA) systems, among others, under mild conditions, see [25]. By considering hybrid dynamical systems in discrete-time a number of mathematical problems (like *Zeno behavior*, see [26], [2]) are avoided and allows to derive models for which tractable analysis and optimal/predictive control techniques exist.

MLD systems are described by linear dynamic equations subject to linear mixed-integer inequalities, i.e., inequalities involving both continuous and binary (or logical, or 0-1) variables. These include physical/discrete states, continuous/integer inputs, and continuous/binary auxiliary variables. The general MLD form is [7]:

$$x(k+1) = Ax(k) + B_1 u(k) + B_2 \delta(k) + B_3 z(k) \tag{1a}$$

$$y(k) = Cx(k) + D_1 u(k) + D_2 \delta(k) + D_3 z(k) \tag{1b}$$

$$E_2 \delta(k) + E_3 z(k) \leq E_1 u(k) + E_4 x(k) + E_5 \tag{1c}$$

The meaning of the variables is the following:

- x are the continuous and binary states:

$$x = \begin{bmatrix} x_c \\ x_\ell \end{bmatrix}, \quad x_c \in \mathbb{R}^{n_c}, \quad x_\ell \in \{0,1\}^{n_\ell} \tag{2}$$

- y are the continuous and binary outputs:

$$y = \begin{bmatrix} y_c \\ y_\ell \end{bmatrix}, \quad y_c \in \mathbb{R}^{p_c}, \quad y_\ell \in \{0,1\}^{p_\ell} \tag{3}$$

- u are the continuous and binary inputs:

$$u = \begin{bmatrix} u_c \\ u_\ell \end{bmatrix}, \quad u_c \in \mathbb{R}^{m_c}, \quad u_\ell \in \{0,1\}^{m_\ell} \tag{4}$$

- Auxiliary binary variables: $\delta \in \{0,1\}^{r_\ell}$
- Auxiliary continuous variables: $z \in \mathbb{R}^{r_c}$.

Notice that by removing (1c) and by setting δ and z to zero, (1a) and (1b) reduce to an unconstrained linear discrete time system. The variables δ and z are introduced when translating logic propositions into linear inequalities. All constraints are summarized in the inequality (1c).

The transformation of certain hybrid system descriptions into the MLD form requires the application of a set of given rules. To avoid the tedious procedure of deriving the MLD form by hand, a compiler was developed in [51] to automatically generate the matrices A, B_i, C, D_i and E_i in (1) through the specification language HYSDEL (HYbrid System DEscription Language).

1.3 MPC and Hybrid Systems

Different methods for the analysis and design of hybrid control systems have been proposed in the literature during the last few years [7], [31], [13]. One of the most studied techniques involves optimal control and related variants such as *hybrid MPC* (HMPC). The formulation of the optimization problem in hybrid MPC follows the approach in standard linear MPC design; see [32]. The desired performance variables are expressed as affine functions of the control variables, initial states and known disturbances. However, due to the Boolean auxiliary variables present, the resulting optimization problem is a *mixed integer quadratic* or *linear program* (MIQP or MILP, respectively). The control law obtained in this way is also referred to as *mixed integer predictive control*.

In general, the HMPC structure is defined by the following optimal control problem. Assume that the hybrid system output should track a reference signal y_r and x_r, u_r, z_r are desired references for the states, inputs and auxiliary variables, respectively. For a fixed prediction horizon H_p, the sequences

$$\begin{aligned} \mathbf{x}_k &= \{x(1|k), x(2|k), \ldots, x(H_p|k)\} \\ \mathit{\Delta}_k &= \{\delta(0|k), \delta(1|k), \ldots, \delta(H_p-1|k)\} \\ \mathbf{z}_k &= \{z(0|k), z(1|k), \ldots, z(H_p-1|k)\} \end{aligned} \tag{5}$$

are generated applying the input sequence $\mathbf{u}_k = \{u(0), u(1), \ldots, u(H_p-1)\}$ to system (1) from initial state $x(0|k) \triangleq x(k)$, where $x(k)$ is the measurement of the current state.

Hence, using the previous concepts, the HMPC optimal control problem is defined as:

$$\min_{\mathbf{u}_k,\Delta_k,\mathbf{z}_k} J\left(\mathbf{u}_k,\Delta_k,\mathbf{z}_k,x(k)\right) \triangleq \left\|Q_{xf}\left(x(H_p|k)-x_f\right)\right\|_p + \sum_{i=1}^{H_p-1}\left\|Q_x\left(x(i|k)-x_r\right)\right\|_p + \sum_{i=0}^{H_p-1}\left\|Q_u\left(u(i)-u_r\right)\right\|_p + \sum_{i=0}^{H_p-1}\left\|Q_z\left(z(i|k)-z_r\right)\right\|_p + \sum_{i=0}^{H_p-1}\left\|Q_y\left(y(i|k)-y_r\right)\right\|_p \tag{6a}$$

$$\text{s. t.} \begin{cases} x_{(0|k)} = x(k), \\ x_f = x_r(H_p|k), \\ x(i+1|k) = Ax(i|k)+B_1u(i)+B_2\delta(i|k)+B_3z(i|k), \\ y(i|k) = Cx(i|k)+D_1u(i)+D_2\delta(i|k)+D_3z(i|k), \\ E_2\delta(i|k)+E_3z(i|k) \leq E_1u(i)+E_4x(i|k)+E_5, \\ \text{for} \quad i=0,1,\cdots,H_p-1 \end{cases} \tag{6b}$$

where $J(\cdot)$ is the cost function and x_f corresponds to the final desired value for the state variable over H_p. p is related to the selected cost norm (i.e., 1-norm, Euclidean or infinity).

Assuming that the HMPC problem (6) is *feasible* for $x(k)$, there exists an optimal solution given by the sequence

$$\mathbf{u}_k^* = \{u^*0), u^*(1), \cdots, u^*H_p-1)\}$$

Then, the *receding horizon control* philosophy sets [32], [15]

$$u_{\text{MPC}}(x(k)) \triangleq u^*(0) \tag{7}$$

and disregards the computed inputs $u^*(1)$ to $u^*(H_p-1)$. The whole process is repeated at the following time step. Equation (7) is known in the MPC literature as *the MPC control law*. The equality constraint related to the final state within the HMPC problem (6) can be relaxed so that $x(H_p|k)$ is only required to belong to a terminal constraint set $\mathbb{X}_T$, [28].

Thus, the HMPC problem (6) is defined by a cost function J in (6a), which is given by the problem control objectives, and by a set of constraints in (6b).

2 Hybrid Modeling and Control of Sewage Systems

2.1 Mathematical Modeling Principles

The water flow in sewer pipes is *open-channel*. Open-channel flow is the flow of a certain fluid in a channel in which the fluid shares a free surface with an empty space above. The Saint-Venant equations[3], based on physical principles of mass conservation and energy, allow the accurate description of the open-channel flow in sewer pipes [36]. These equations are expressed as:

$$\frac{\partial q(x,t)}{\partial x} + \frac{\partial A(x,t)}{\partial t} = 0 \tag{8}$$

$$\frac{\partial q(x,t)}{\partial t} + \frac{\partial}{\partial x}\left(\frac{q(x,t)^2}{A(x,t)}\right) + gA(x,t)\frac{\partial L(x,t)}{\partial x} - gA(x,t)\left(I_0-I_f\right) = 0 \tag{9}$$

[3] Adhémar Jean Claude Barré de Saint-Venant (1797 - 1886) was a mechanician who developed the one-dimensional unsteady open channel flow equations for shallow water or Saint-Venant equations that are a fundamental set of equations in modern hydraulic engineering.

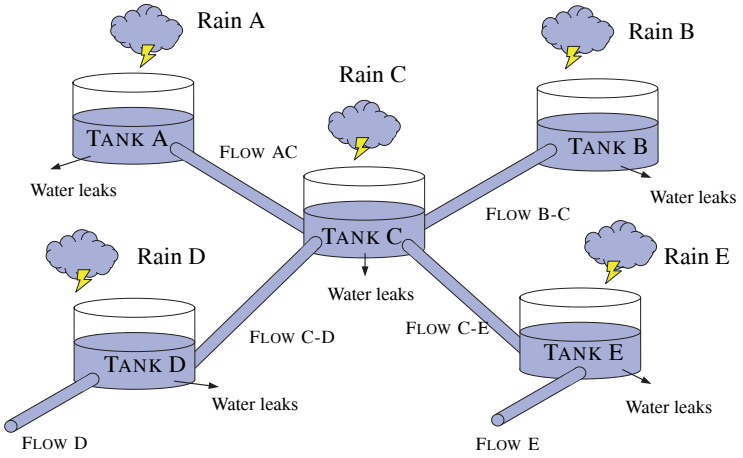

Fig. 1. Sewer network modeling by means of *virtual tanks*

where $q(x,t)$ is the flow (m^3/s), $A(x,t)$ is the cross-sectional area of the pipe (m^2), t is the time variable (s), x is the spatial variable measured in the direction of the sewage flow (m), g is the gravity (m/s^2), I_0 is the sewer pipe slope (dimensionless), I_f is the friction slope (dimensionless) and $L(x,t)$ is the water level inside the sewer pipe (m). This pair of partial-differential equations constitutes a non-linear hyperbolic system. For an arbitrary geometry of the sewer pipe these equations lack an analytical solution. Notice that these equations describe the system behavior in high detail. However, such a level of detail is not useful for real-time control implementation due to the complexity of obtaining the solution of (8)-(9) and the associated high computational cost.

Alternatively, several modeling techniques have been presented in the literature that deal with real-time sewer system control, see [33], [21], [19], [34], among many others. The modeling approach used in this chapter is close to the approach presented in [22]. Here, the sewer system is divided into catchments which are treated as *virtual tanks* (see Fig. 1). At any given time, the stored volumes represent the amount of water inside the sewer pipes associated with the tank and are calculated on the basis of the rainfall of the catchment area of the tank and flow exchanges between other interconnected virtual tanks. The volume is calculated through the mass balance of the stored volume, the inflows and the outflow of the tank and the input rain intensity. The mentioned mass balance can be written as the difference equation

$$v_i(k+1) = v_i(k) + \Delta t \varphi_i S_i P_i(k) + \Delta t \left(q_i^{\text{in}}(k) - q_i^{\text{out}}(k) \right) \tag{10}$$

where φ_i is the *ground absorption coefficient* of the *i-th* tank catchment, S is the surface area of the *i-th* tank catchment, Δt is the time interval between measurements and P is the *rain intensity* corresponding to the *i-th* tank catchment in Δt time units. $q_i^{\text{in}}(k)$ and $q_i^{\text{out}}(k)$ are the sum of inflows and outflows, respectively. *Real retention tanks* are modeled in the same way but without the precipitation term.

The tanks (either, real or virtual) are connected with flow paths or links which corresponds to the main sewage pipes between the tanks. Figure 2 gives an idea of the interrelation between different components of a very simple sewer network using the proposed modeling methodology. The tank outflows are generally assumed to be a function of the tank volume. For the

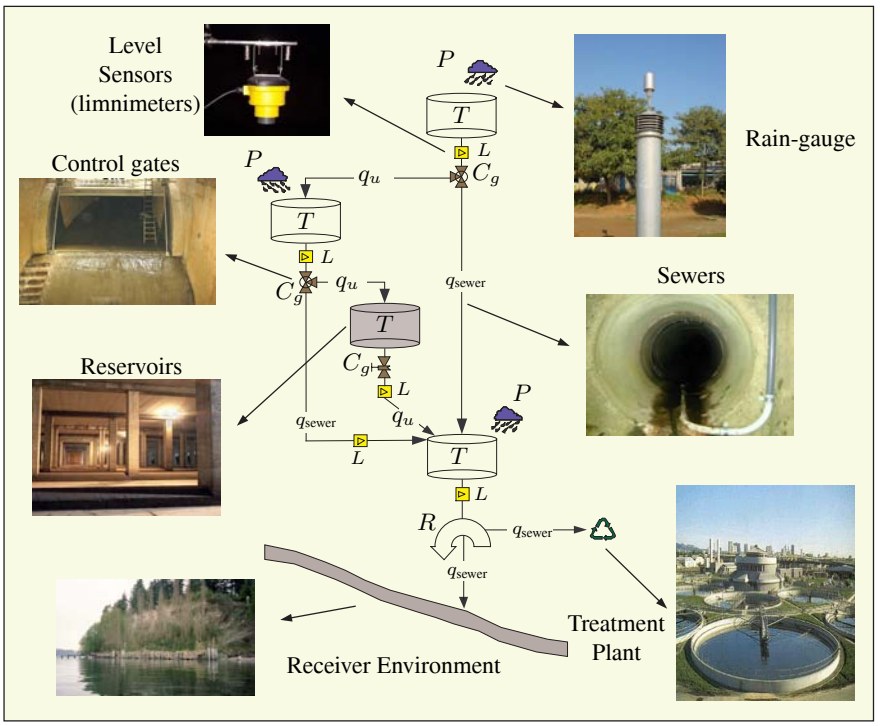

Fig. 2. Components for a basic scheme of a sewer network

current application a linear relation has been assumed, that is,

$$q_i^{\text{out}}(k) = \beta_i v_i(k) \tag{11}$$

where β_i (given in s^{-1}) is defined as the *volume/flow conversion coefficient* as suggested in [48].

The manipulated variables of the system, denoted as q_{u_i}, are related to the outflows from the tanks. In the case of a real tank, a *retention gate* is present to control the outflow. Virtual tank outflows can not be closed but can be redirected with *redirection gates* (RG). The redirection gates divert the flow from a nominal flow path which the flow follows if the redirection gate is closed. This nominal flow is denoted as Q_i in the equation below, which expresses mass conservation at the redirection gate:

$$q_i^{\text{out}}(k) = Q_i(k) + \sum_j q_{u_i}^j(k) \tag{12}$$

where j is an index over all manipulated flows coming from the redirection gate. The flow path which Q_i represents is assumed to have a certain capacity and when this capacity reaches its limits, an overflow situation occurs. This flow limit will be denoted $\overline{Q}_i$. When Q_i reaches its capacity, two cases are considered: first, the water starts to flow on the streets, causing an overflow situation and secondly, it exits the sewer network and is considered lost to the

environment. In the first case, the overflow water either follows the nominal flow path and ends up in the same tank as Q_i or it is diverted to an other virtual tank. Flow to the environment physically represents the situation when the sewage water ends up in a river or, in the case of the Barcelona situation, in the Mediterranean sea.

When using this modeling approach where the inherent nonlinearities of the sewer network are simplified by assuming that only flow rates are manipulated, physical restrictions need to be included as constraints on system variables. For example, the manipulated variables $q^j_{u_i}$ that determine the redirection of an outflow from a tank should never be larger than the nominal outflow from the tank given by (11). This is expressed with the following inequality

$$\sum_j q^j_{u_i}(k) \leq q^{out}_i(k) \tag{13}$$

Usually the range of actuation is also limited so that the manipulated variable has to fulfill $\underline{q}^j_{u_i} \leq q^j_{u_i}(k) \leq \overline{q}^j_{u_i}$, where $\underline{q}_{u_i}$ denotes the lower limit of manipulated flow and $\overline{q}_{u_i}$ denotes its upper limit. When $\underline{q}^j_{u_i}$ equals zero, this constraint is convex. But, if the lower bound is larger than zero, a constraint representing mass conservation has to be included in the range limitation leading to the following non-convex inequality:

$$\min(\underline{q}^j_{u_i}, q^{out}_i(k) - \sum_{t \neq j} q^t_{u_i}(k)) \leq q^j_{u_i}(k) \leq \overline{q}^j_{u_i} \tag{14}$$

The sum in the expression is calculated for all outflows related to tank i except j.

A further complication is that if the control signal is an inflow to a real tank that has hard constraints on its capacity, then the situation can occur that this lower limit is also limited by this maximum capacity and the outflow from the real tank. The limit on the range of real tanks is expressed as

$$0 \leq v_i(k) \leq \overline{v}_i \tag{15}$$

where $\overline{v}_i$ denotes the maximum volume capacity given in m^3. As this constraint is physical, it is impossible to send more water to a real tank than it can hold.

The virtual tanks do not have a physical limit on their capacity. When they rise above a decided level an overflow situation occurs. This represents the case when the level in the sewers has reached a limit so that an overflow situation can occur in the streets. Notice that in practice, the difference between tank and link overflows is often small.

Model Calibration from Real Data

Real data from sensor measurements were used to estimate the parameters of the virtual tanks. Level is measured in sewer pipes using ultrasonic limnimeters. Notice that the sewer level is measured instead of the flow through the sewer. As these level sensors have no contact with the water flow, problems due to incorrect measurements caused by sensor faults are avoided. From these level measurements, the flow entering and exiting each virtual tank can be estimated assuming steady-uniform flow using the *Manning formula*[4] [36]:

$$q = vS_w \tag{16}$$

[4] The Manning formula is an empirical formula for open channel flow, or flow driven by gravity. It was developed by the French engineer *Robert Manning* and proposed on 1891 in the Transactions of the Institution of Civil Engineers (Ireland).

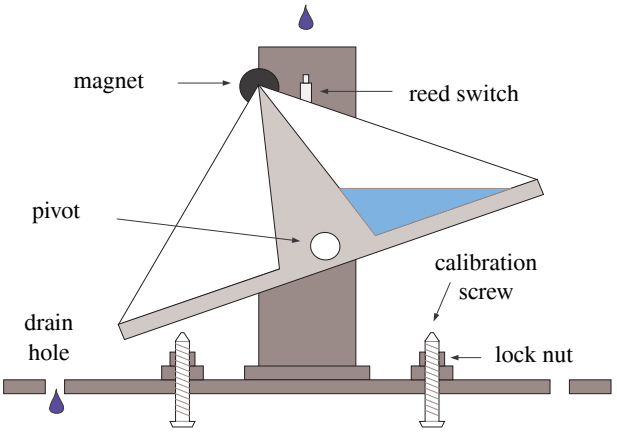

Fig. 3. Rain measurement principle using a tipping-bucket rain-gauge

where S_w is the *wetted surface* that depends on the cross-sectional sewer area A and water level L within the sewer. The dependence of A and L on x and t are omitted for compactness. Moreover, v is the water velocity computed according to the parameters relation

$$v = \frac{K_n}{n} R_h^{2/3} I_0^{1/2} \tag{17}$$

where K_n is a constant whose value depends of the measurement units used in the equation, n is the Manning coefficient of roughness which depends of flow resistance offered by the sewer pipe material, R_h is the hydraulic radius defined as the relation of the cross sectional area of flow and the wetted perimeter P_w as $R_h = A/P_w$, and I_0 is the sewer slope. For a given geometry of the sewer cross-section, wetted perimeter and hydraulic radius can be expressed in terms of the sewer level L. For instance, given a rectangular cross-section of width b, the wetted surface S_w is bL, the wetted perimeter P_w is $b + 2L$ and the hydraulic radius is given by $R_h = \frac{bL}{b+2L}$.

Rain intensity is measured using a *tipping bucket rain-gauge* (see Fig. 3). This gauge technology uses two small *buckets* mounted on a fulcrum (balanced like a see-saw). The tiny buckets are manufactured with tight tolerances to ensure that they hold an exact amount of precipitation. The tipping bucket assembly is located above the rain sewer, which funnels the precipitation to the buckets. As rainfall fills the tiny bucket, it becomes overbalanced and tips down, emptying itself as the other bucket pivots into place for the next reading. The action of each tipping event triggers a small switch that activates the electronic circuitry to transmit the count to the indoor console, recording the event as 1.2 mm/h of rainfall. The number of tipping events in 5 minutes (sampling time) is accumulated and multiplied by 1.2 mm/h in order to obtain the rain intensity P in m/s at each sampling time, after the appropriate units conversion.

Given rain intensities as well as limnimeter data, data series with P_i and input/output flows can be determined. By combining (10) and (11), the following input/ouput equation in function of the flow in sewers and rain intensity in catchments can be obtained:

$$q_i^{out}(k+1) = a q_i^{out}(k) + b_1 P_i(k) + b_2 q_i^{in}(k) \tag{18}$$

where $a = (1 - \beta_i \Delta t)$, $b_1 = \beta_i \Delta t \varphi_i S_i$ and $b_2 = \beta_i \Delta t$. Figure 4 represents this equation and the interaction of all described parameters and measurements.

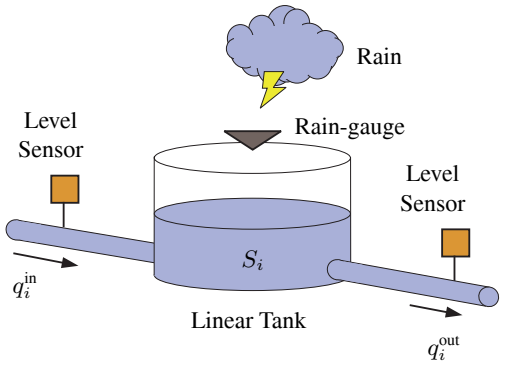

Fig. 4. Scheme of an individual virtual tank and its parameters and measurements

Equation (18) is linear in the parameters. This allows the parameters to be estimated using classical parameter estimation methods based on *least-squares algorithms* [30]. Hence, the parameter associated with the ground absorption coefficient is estimated as

$$\varphi_i = \frac{b_1}{b_2 S_i} \tag{19}$$

and the volume/flow conversion coefficient is estimated as

$$\beta_i = \frac{b_2}{\Delta t} \tag{20}$$

for the *i-th* catchment.

Ground absorption and volume/flow conversion coefficients can be estimated on-line at each sampling time using (18) and the recursive least-squares (RLS) algorithm [30]. Once estimated, these parameters are supplied to the MPC controller in order to take into account their time variation and neglected non-linearities.

2.2 Hybrid Modeling of Sewer Systems

The presence of intense precipitation can cause some sewers to reach their limits of capacity. When this happens, excess sewage that normally would have been collected in the sewer can flow to to other parts of the sewer system. In this way, as mentioned in Sect. 1, flow paths appear that are not always present and depend on the system state and inputs.

This behavior and other particular hybrid phenomena of sewer systems that depend on system state can be conveniently modeled using the discrete time hybrid dynamical models introduced in Sect. 1. In what follows it will be shown how some common elements of sewer systems can be represented with these models. Specifically, the elements that will be considered are virtual tanks, flow links and redirection gates. Other common sewer system elements such as pumping stations can be easily modeled within the hybrid modeling methodology but will be omitted as they do not occur in the case study presented later. Hybrid dynamic behavior in sensors such as rain gauges and limnimeters is also omitted.

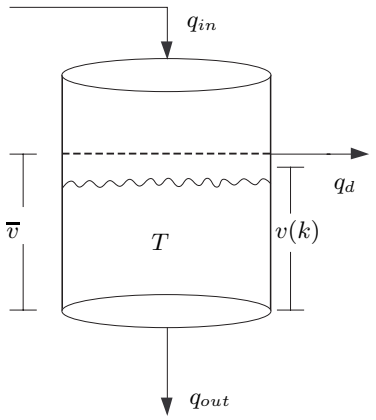

Fig. 5. Scheme of a virtual tank

Virtual tanks (VT)

When the maximum volume $\overline{v}$ in virtual tanks is reached, the excess volume above this maximum amount is redirected to another tank within the network. This creates a new outflow from the tank denoted with q_d in Fig. 5. This phenomenon can be expressed mathematically as:

$$q_d(k) = \begin{cases} \frac{(v(k)-\overline{v})}{\Delta t} & \text{if} \quad v(k) \geq \overline{v} \\ 0 & \text{otherwise} \end{cases} \tag{21a}$$

$$q_{out}(k) = \begin{cases} \beta\overline{v} & \text{if} \quad v(k) \geq \overline{v} \\ \beta v(k) & \text{otherwise} \end{cases} \tag{21b}$$

where $v(k)$ corresponds to the tank volume (system state), $\overline{v}$ is its maximum volume capacity, Δt is the sampling time and β is a proportional factor between the volume and the outflow, see [38]. The flow q_d is referred to as *virtual tank overflow*. The difference equation for the virtual tank is

$$v(k+1) = v(k) + q_{in}(k) - q_{out}(k) - q_d(k) \tag{22}$$

Redirection gates (RG)

These type of elements within a sewer network are used to redirect flow at a certain point in the network. An inflow q_{in} is redirected to outflows q_a and q_b as shown in Fig. 6. Two types of redirection elements are considered. In the first type referred to as passive (also know as weirs), the flow follows the path q_a until a limit $\overline{q}_a$ is reached. If q_{in} is larger than $\overline{q}_a$ then the difference flows through q_b. In the other type, flow q_a can be manipulated within its physical limits. The expressions for the first type of redirection gates are:

$$q_a(k) = \begin{cases} q_{in}(k) & \text{if} \quad q_{in} \leq \overline{q}_a \\ \overline{q}_a & \text{otherwise} \end{cases} \tag{23a}$$

$$q_b(k) = q_{in}(k) - q_a(k) \tag{23b}$$

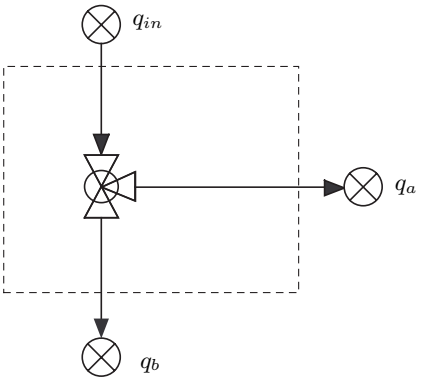

Fig. 6. Scheme of redirection gate element

while in the second type, since the flow q_a is manipulated, the flow only has to fulfill the following restrictions:

$$0 \leq q_a(k) \leq q_{in} \tag{24a}$$
$$q_a(k) \leq \overline{q}_a \tag{24b}$$
$$q_a(k) = q_{in}(k) - q_b(k) \tag{24c}$$

Flow links (FL)

The outflow from virtual tanks is assumed to be unlimited to guarantee a feasible solution. The same thing applies to the outflow q_b from the retention gate element. But most often flow links between elements in the sewer network have limited flow capacity. The flow link element serves to model this limited capacity. When the limit of flow capacity is exceeded, the resulting overflow is possibly redirected to another element in the system or is considered lost to the environment. The overflow is denoted q_c in Fig. 7. The equations for the flow link are:

$$q_b(k) = \begin{cases} \overline{q}_b & \text{if} \quad q_{in} > \overline{q}_b \\ q_{in}(k) & \text{otherwise} \end{cases} \tag{25a}$$
$$q_c(k) = \begin{cases} q_{in}(k) - \overline{q}_b & \text{if} \quad q_{in} > \overline{q}_b \\ 0 & \text{otherwise} \end{cases} \tag{25b}$$

where $\overline{q}_b$ is the maximum flow through q_b and q_{in} is the inflow to the flow link.

The hybrid sewer system model

The total sewer system model is constructed by connecting the system inflows (rain) and outflows (sewer treatment plants or outflows to the environment) with the inflows and outflows

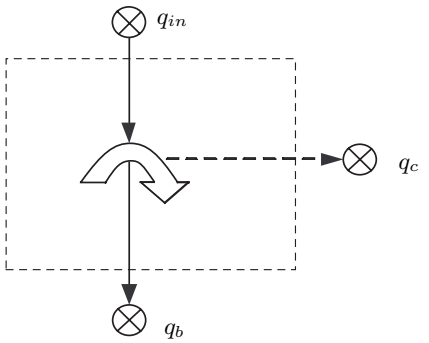

Fig. 7. Scheme for flow links

of the elements as well as connecting the elements themselves. The manipulated variables of the system, denoted as q_u, are the manipulated variables of each component as described before. The logical conditions presented to describe the dynamics of the sewer system elements can be translated into linear integer inequalities as described in [7]. The whole sewer network expressed in MLD form can be written as:

$$v(k+1) = Av(k) + B_1 q_u(k) + B_2\delta(k) + B_3 z(k) + B_4 d(k) \tag{26a}$$
$$y(k) = Cv(k) + D_1 q_u(k) + D_2\delta(k) + D_3 z(k) + D_4 d(k) \tag{26b}$$
$$E_2\delta(k) + E_3 z(k) \leq E_1 q_u(k) + E_4 v(k) + E_5 + E_6 d(k) \tag{26c}$$

where $v \in \mathbb{R}_+^{n_c}$ corresponds to the vector of tank volumes (states), $q_u \in \mathbb{R}_+^{mi_c}$ is the vector of manipulated sewer flows (inputs), $d \in \mathbb{R}_+^{md}$ is the vector of rain measurements (disturbance), logic vector $\delta \in \{0,1\}^{r_\ell}$ collects the boolean overflow conditions and vector $z \in \mathbb{R}_+^{r_c}$ is associated with variables that appear depending on system states and inputs. Variables δ and z are auxiliary variables associated with the MLD form. Equation (26c) collects the set of element constraints as well as translations from logic propositions. Notice that this model is a more general MLD than was presented in [7] due to the addition of the measured disturbances.

If it is assumed that the disturbances are described with a disturbance model $d(k+1) = A_d d(k)$, the MLD (26) form could be rewritten as:

$$v(k+1) = \begin{bmatrix} A & B_4 \\ 0 & A_d \end{bmatrix} \begin{bmatrix} v(k) \\ d(k) \end{bmatrix} + \begin{bmatrix} B_1 & B_2 & B_3 \end{bmatrix} \begin{bmatrix} q_u(k) \\ \delta(k) \\ z(k) \end{bmatrix} \tag{27a}$$

$$y(k) = \begin{bmatrix} C & C_d \end{bmatrix} \begin{bmatrix} v(k) \\ d(k) \end{bmatrix} + \begin{bmatrix} D_1 & D_2 & D_3 \end{bmatrix} \begin{bmatrix} q_u(k) \\ \delta(k) \\ z(k) \end{bmatrix} \tag{27b}$$

$$\begin{bmatrix} E_2 & E_3 \end{bmatrix} \begin{bmatrix} \delta(k) \\ z(k) \end{bmatrix} \leq \begin{bmatrix} E_4 & E_6 \end{bmatrix} \begin{bmatrix} v(k) \\ d(k) \end{bmatrix} + \begin{bmatrix} E_1 & E_5 \end{bmatrix} \begin{bmatrix} q_u(k) \\ 1 \end{bmatrix} \tag{27c}$$

The type of model to be used for disturbance $d(k)$ in sewer system control is, in general, an open research topic. Different types of rain prediction models can be used (statistical, AR

models, etc) [49] or the rain precipitation can be measured and predicted more directly (radars, meteorological satellites, etc) [53]. Combinations of the two approaches have also been presented. According to [16], when an optimal control law is used in the RTC of sewer networks with a short prediction horizon, assuming that the rain is constant over the prediction horizon results in a moderate performance loss compared to knowing exactly the rain over the horizon. This confirmed similar results reported in [22]. For constant rain over the prediction horizon, matrix A_d is set as the identity matrix of suitable dimensions.

2.3 The Hybrid Control Strategy

As discussed in previous section, the proposed hybrid modeling methodology is very rich and allows the straightforward treatment of hybrid phenomena such as overflow and flooding. Morever, HMPC has been applied successfully to a variety of control problems the last years using several approaches, see [14], [47], [50], [29], [5], among others. This section presents a description of the HMPC formulation applied on sewer networks. The different aspects discussed here are presented considering the particular case study but can be easily extrapolated to other sewage systems topologies. The concepts and definitions of Sect. 1.3 are applied in this section in a straightforward manner but taking into account the particular notation used for sewer networks.

Control objectives

The sewer system control problem has multiple objectives with varying priority, see [34]. There exist many types of objectives according to the system design. In general, the most common objectives are related to the manipulation of the sewage in order to avoid undesired sewage overflow on the streets of the city. Other kind of objectives are for instance related to the control energy, i.e., the energy cost of the regulation of the gate movements. According to the literature of sewer networks, the main objectives for the case study of this chapter are listed below in order of decreasing priority:

- *Objective 1:* minimize flooding in streets (virtual tank overflow).
- *Objective 2:* minimize flooding in links between virtual tanks.
- *Objective 3:* maximize sewage treatment.
- *Objective 4:* minimize control action.

A secondary purpose of the third objective is to reduce the volume in the tanks to anticipate future rainstorms. This objective also indirectly reduces pollution to the environment. This is because if the treatment plants are used optimally along with the storage capacity of the network, pollution lost to the environment should be at a minimum. It should be noted that in practice the difference between the first two objectives is small. According to the hybrid model for sewer networks proposed in Sect. 2.2, all overflows and flows to treatment plants are defined by auxiliary variables z. However, as some of the performance objectives are sums of system variables, it is convenient to define system outputs where these sums are calculated.

The cost function

Each control objective corresponds to one term in the cost function. Hence, the expression of that function depends on its constitutive variables (auxiliary or output type). In general form, the structure for the cost function in (6a) has the form

$$J(\mathbf{u}_k, v(k)) \triangleq \sum_{i=0}^{H_p-1} \|Q_z(z_{(k+i|k)} - z_r)\|_p + \sum_{i=0}^{H_p-1} \|Q_y(y_{(k+i|k)} - y_r)\|_p \qquad (28)$$

where Q_z and Q_y correspond to weight matrices of suitable dimensions and z_r, y_r are reference trajectories related to auxiliary and output variables, respectively. For the objectives 1-2, the references are zero flow. For the third objective, the references are the maximum capacity of the associated sewage treatment plants. Priorities are set by selecting matrices Q_z and Q_y. The norm p can be selected as $p = 1, 2$ or $p = \infty$. Notice that due to the fact that all performance variables are positive, the case when $p = 1$ is actually a simple sum of the performance variables.

2.4 Case Study Description

The Barcelona sewer network

The city of Barcelona has a combined sewage system of approximately 1697 Km length with a storage capacity of 3038622 m^3. It is a unitary system, that is, it combines waste and rainwater into the same sewers. It is worth to notice that Barcelona has a population, which is approximately around 1593000 inhabitants on a surface of 98 Km^2, resulting in a very high density of population. Additionally, the yearly rainfall is not very high (600 mm/year), but it includes heavy storms (arriving to 90 mm/h) typical of the Mediterranean climate that can cause a lot of flooding problems and CSO to the receiving waters.

Clavegueram de Barcelona, S.A. (CLABSA) is the company in charge of the sewer system management in Barcelona. There is a remote control system in operation since 1994 which includes, sensors, regulators, remote stations, communications and a Control Center in CLABSA. Nowadays, for control purposes, the urban drainage system contains 21 pumping stations, 36 gates, 10 valves and 8 detention tanks which are regulated in order to prevent flooding and CSO. The remote control system is equipped with 56 remote stations including 23 rain-gauges and 136 water-level sensors which provide real-time information about rainfall and water levels into the sewer system (see Fig. 8). All this information is centralized at the CLABSA Control Center through a supervisory control and data acquisition (SCADA) system. The regulated elements (pumps, gates and detention tanks) are currently controlled locally, i.e., they are handled from the remote control center according to the measurements of sensors connected only to the local station.

Barcelona test catchment

In this chapter, a representative portion of the Barcelona sewer system is studied. Figure 9 shows the catchment over a real map of Barcelona. A calibrated and validated model of the system following the methodology explained in Sect. 2.1 is available as well as rain gauge data for an interval of several years.

The catchment has a surface of 22.6 Km^2 and includes typical elements of the larger network. Due to its size, there is a spacial difference in the rain intensity between rain gauges. The system is presented in Fig. 11 using the virtual reservoir methodology presented in Sect. 2.1. The catchment area considered has 1 retention gate associated with 1 real tank, 3 redirection gates, 11 sub-catchments defining the same number of virtual tanks, several limnimeters and a pair of links connected to the same number of treatment plants. Also there are 5 rain-gauges in the catchment but some virtual tanks share the same rain sensor. The difference between

Fig. 8. CLABSA Control Center

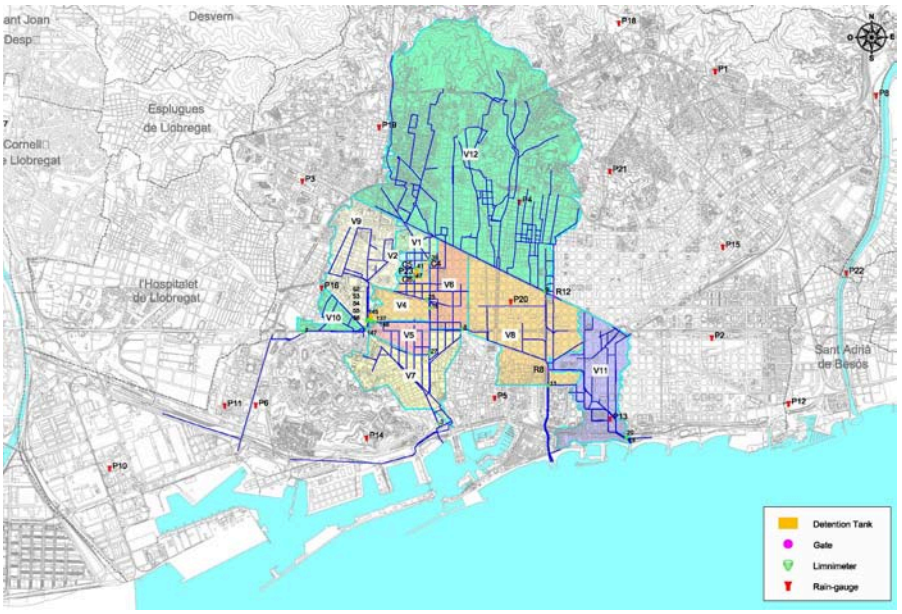

Fig. 9. Test Catchment located over the Barcelona map (Courtesy of CLABSA)

the rain inflows for virtual tanks that share a sensor lies in the surface area A and the ground absorbtion coefficient φ. This results in a different amount of rain entering to the virtual tank even though the rain intensity is the same. The real tank corresponds to the *Escola Industrial* reservoir, which is located under a soccer field of the Industrial School of Barcelona (see Fig. 10). It has a rectangle geometry of 94×54 m with a medium depth of 7 m and a maximum water capacity of 35000 m^3 [18].

Fig. 10. Retention tank located at Escola Industrial de Barcelona

The related system model has 12 state variables corresponding to the volumes in the 12 tanks (1 real, 11 virtual), 4 control inputs and 5 measured disturbances corresponding to the measurements of rain intensity over the virtual tanks. Two water treatments plants can be used to treat the sewer water before it is released to the environment. It is supposed that all states (virtual tank volumes) are estimated by using the limnimeters shown with capital letter L in Fig. 11. The flows to the environment as pollution, ($q_{10\mathrm{M}}$, $q_{7\mathrm{M}}$, $q_{8\mathrm{M}}$ and $q_{11\mathrm{M}}$ to the Mediterranean sea and q_{12s} to an other catchment) and the flows to the treatment plants ($Q_{7\mathrm{L}}$ and $Q_{11\mathrm{B}}$) are shown in the figure as well. Also appearing in the figure are the rain intensities P_{13}, P_{14}, P_{16}, P_{19} and P_{20}. The 4 controlled flows, denoted as q_{u_i}, $i = 1 \ldots 4$, have a maximum flow capacity of 9.1, 25.0, 7.0 and 29.3 m^3/s, respectively.

Figures 12(a) and 12(b) present the comparison between real level (from real data) and predicted level (using the model described in Sect. 2.1) corresponding to the output flows of virtual tank T_1 and T_2, respectively. It can be noticed that the fit obtained with the proposed modeling approach is satisfactory.

Tables 1 and 2 summarize the description of the case study variables as well as the value of the parameters obtained by calibrating the system model following the procedures described in Sect. 2.1. In Table 1 (and also in Fig. 11), T_i denotes the i-th virtual tank and T_3 denotes the real tank. Moreover, $\overline{v}_i$ denotes the maximum capacity of the i-th tank (virtual or real). Elements R_1 to R_5 denote passive redirection gates. The maximum capacities of the redirection gate flows as well as flow links are given in Table 2.

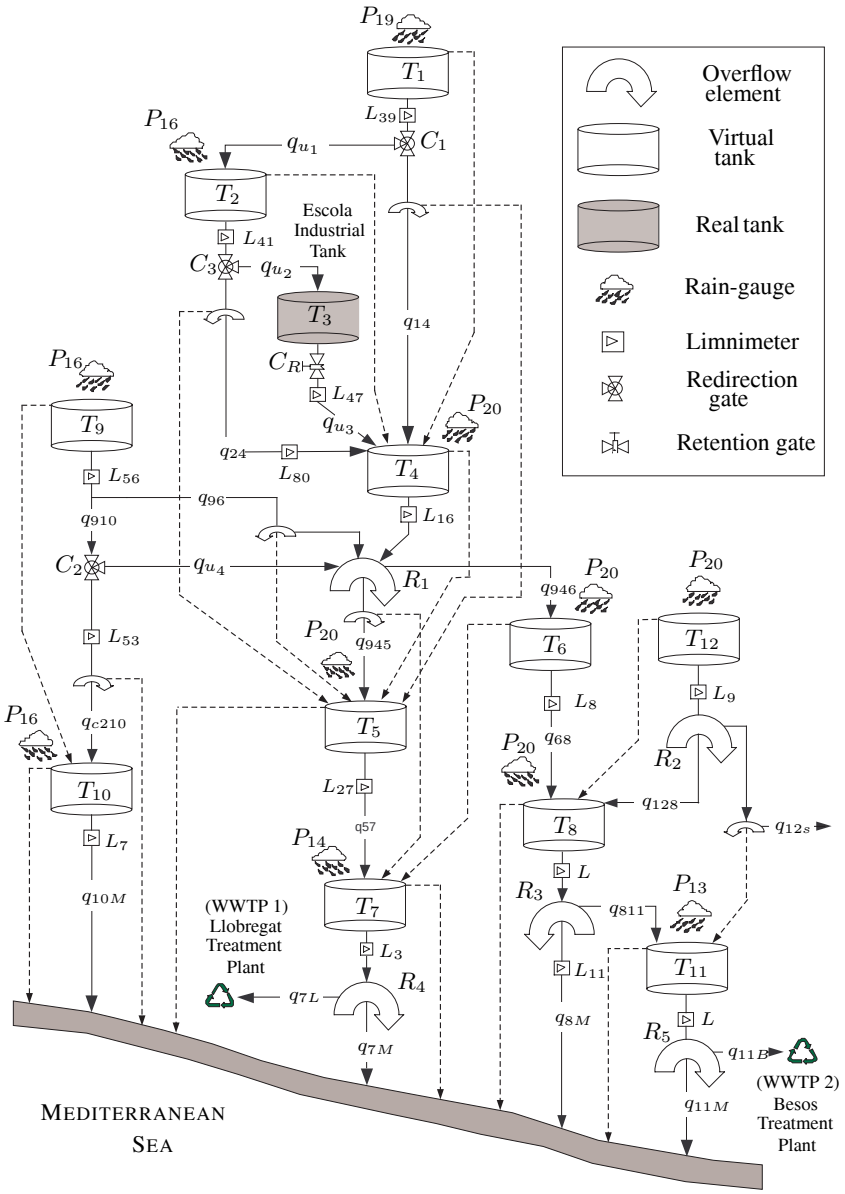

Fig. 11. Scheme of the Barcelona sewer network catchment

3 Simulation and Results

3.1 Rain Episodes

The rain episodes included in the case study are based on real rain gauge data obtained within the city of Barcelona on the given dates (day-month-year) as seen in Table 4. These episodes

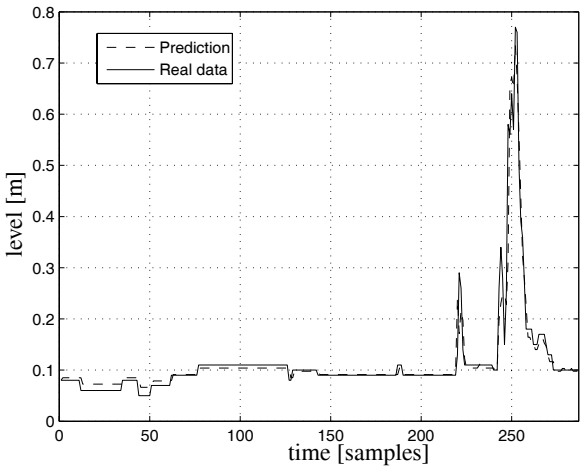

(a) Output level in T_1

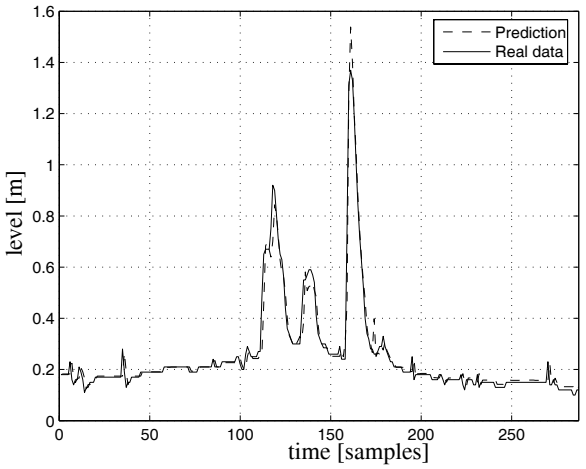

(b) Output level in T_2

Fig. 12. Results of model calibration using the approach given in Sect. 2.1

were selected to represent the meteorological behavior of Barcelona. In Fig. 13, the reading of the rain gauges for one of the rain episodes is shown. The rain storm presented in this figure caused severe flooding in the city area under study.

Table 1. Parameter values related to the sub-catchments within the case study

Tank	S (m^2)	φ_i	β_i (s^{-1})	$\overline{v}_i$ (m^3)
T_1	323576	1.03	7.1×10^{-4}	16901
T_2	164869	10.4	5.8×10^{-4}	43000
T_3	5076	–	2.0×10^{-4}	35000
T_4	754131	0.48	1.0×10^{-3}	26659
T_5	489892	1.93	1.2×10^{-4}	27854
T_6	925437	0.51	5.4×10^{-4}	26659
T_7	1570753	1.30	3.5×10^{-4}	79229
T_8	2943140	0.16	5.4×10^{-4}	87407
T_9	1823194	0.49	1.3×10^{-4}	91988
T_{10}	385274	5.40	4.1×10^{-4}	175220
T_{12}	1913067	1.00	5.0×10^{-4}	91442
T_{12}	11345595	1.00	5.0×10^{-4}	293248

Table 2. Description and maximum flow values of the main sewers in the case study

Sewer	$\overline{q}$ (m^3/s)	Sewer	$\overline{q}$ (m^3/s)
q_{14}	9.14	q_{128}	63.40
q_{24}	3.40	q_{57}	14.96
q_{96}	10.00	q_{68}	7.70
$q_{\mathrm{c}210}$	32.80	$q_{12\mathrm{s}}$	60.00
q_{945}	13.36	q_{811}	30.00
q_{910}	24.00	$q_{7\mathrm{L}}$	7.30
q_{946}	24.60	$q_{11\mathrm{B}}$	9.00

3.2 Results

The purpose of this section is to show the performance of hybrid MPC for realistic episodes of rain storms. The assumptions made for the implementation will be presented and their validity discussed before the results are given.

The transformation of the hybrid system equations into the MLD form requires the application of the set of given rules [7]. The higher level language and associated compiler HYSDEL (see [51]) is used here to avoid the tedious procedure of deriving the MLD form by hand. Given the MLD model, the controllers were designed and the scenarios simulated using the *Hybrid Toolbox* for MATLAB® (see [4]). Moreover, ILOG CPLEX 9.1 has been used for solving the MIP problems.

Simulation of scenarios

The performance of the control scheme is compared with the simulation of the sewer system without control when the manipulated links have been used as passive elements, i.e., the amount of flows $q_{u1}(k)$, $q_{u2}(k)$ and $q_{u4}(k)$ only depend on the inflow to the corresponding gate and they are not manipulated (see Sect. 2.2) while $q_{u3}(k)$ is the natural outflow of the real tank.

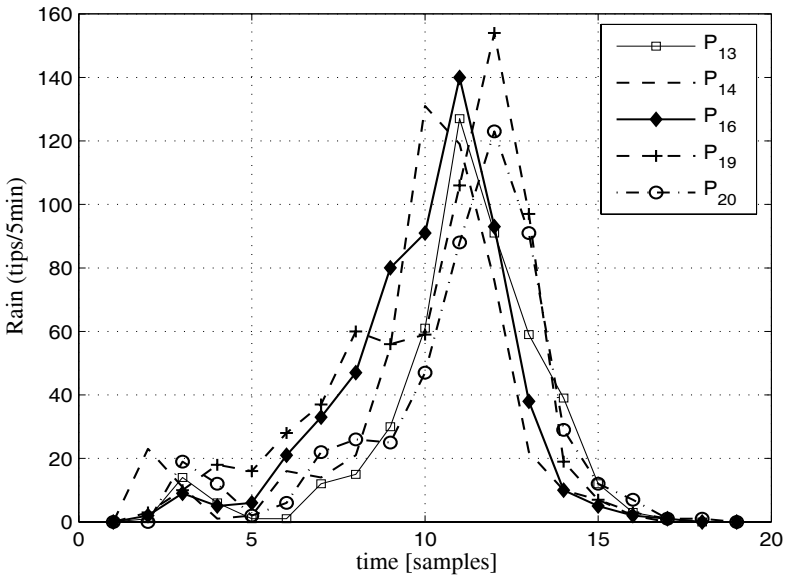

Fig. 13. Example of rain episode occurred in Barcelona on 14 September, 1999. Each curve represents a rain gauge P_i.

Two different MLD models are used to simulate the scenarios, one for the hybrid MPC controller, MLD_C which has been described in Sect. 2 and one tailored for the open loop simulation, MLD_{OL}. The difference lies in the fact that when the system is simulated in open loop, logical conditions have to be added so that the physical constraints of the system are respected. The model MLD_{OL} is therefore augmented so that the control signals from the controller are adjusted to respect the physical restrictions of the whole network. MLD_{OL} contains more auxiliary variables for this reason.

The MLD_C model implemented has 22 logical variables and 44 auxiliary variables. The prediction horizon H_p was set to 6 which is equivalent to 30 minutes (with the sampling time $\Delta t = 300s$, 5 min). The length of the simulation scenarios is 100 samples. The computation times presented in Sect. 4 were obtained on a INTEL® PENTIUM® M 1.73 GHz machine.

The control tuning is done taking into account the prioritization of the control objectives. In a preliminary study, different norms, cost function structures and cost function weights w_i have been used. In order to give a hierarchical priority to the control objectives, the relation of w_i between objectives is an order of magnitude.

Table 5 relates the auxiliary variables z with the control objectives discussed in Sect. 2.3. A suitable norm for the first objective is the ∞-norm. This minimizes the worst case street flooding at each sample. On the other hand, for the second objective, the 1-norm is more suitable. As the variables are all positive, the following outputs are defined to implement the 1-norm indirectly with the ∞-norm based cost function

Table 3. Relation between z variables and control objectives

Objective	z vector	z variable	Description
1	z_{str_v}	z_2	overflow in T_1
		z_6	overflow in T_2
		z_{10}	overflow in T_4
		z_{12}	overflow in T_9
		z_{20}	overflow in T_5
		z_{22}	overflow in T_6
		z_{24}	overflow in T_7
		z_{26}	overflow in T_{12}
		z_{32}	overflow in T_8
		z_{36}	overflow in T_{10}
		z_{40}	overflow in T_{11}
2	z_{str_q}	z_4	overflow in q_{14}
		z_8	overflow in q_{24}
		z_{14}	overflow in q_{96}
		z_{18}	overflow in q_{945}
		z_{30}	overflow in $q_{12\text{s}}$
		z_{34}	overflow in q_{c210}
3	z_{sea}	z_{29}	flow to environment ($q_{12\text{s}}$)
		z_{35}	flow to sea ($q_{10\text{M}}$)
		z_{38}	flow to sea ($q_{8\text{M}}$)
		z_{42}	flow to sea ($q_{11\text{M}}$)
		z_{44}	flow to sea ($q_{7\text{M}}$)
4	—	z_{43}	flow to Llobregat WWTP
	—	z_{41}	flow to Besòs WWTP

$$y_1 = \sum_i z_{\text{sea}}(i),$$
$$y_2 = z_{41} \quad \text{and} \quad y_3 = z_{43}$$

Performance Improvement

Taking into account that the system performance in open loop for the considered rain has a flooding volume of 108×10^3, a pollution volume of 225.9×10^3 and a volume of treated water of 278.3×10^3 (all in m^3), the improvement obtained is between 4.5% and 22.1% for the first objective and the other objectives keep almost in the same values for most of the cases, fulfilling the desired objective prioritization.

Table 4 summarizes the results for ten of the more representative rain episodes in Barcelona between 1998 and 2002. The results were obtained considering $p = 2$, a cost function containing only output variables and with the weight of the most important of its terms set as $w_{\text{str}_v} = 10^{-2}$. The system performance in general is improved when the hybrid control strategy is applied (see percentages for some values).

Table 4. Obtained results of closed loop performance using 10 representative rain episodes

Rain Episodes	Open Loop			Closed Loop		
	Flooding $\times 10^3$ (m^3)	Pollution $\times 10^3$ (m^3)	Treated W. $\times 10^3$ (m^3)	Flooding $\times 10^3$ (m^3)	Pollution $\times 10^3$ (m^3)	Treated W. $\times 10^3$ (m^3)
14-09-1999	108	225.8	278.4	92.9 (14%)	223.5	280.7
09-10-2002	116.1	409.8	533.8	97.1 (16%)	398.8	544.9
03-09-1999	1	42.3	234.3	0 (100%)	44.3	232.3
31-07-2002	160.3	378	324.4	139.7 (13%)	374.6	327.8
17-10-1999	0	65.1	288.4	0	58.1 (11%)	295.3
28-09-2000	1	104.5	285.3	1	98 (6%)	291.9
25-09-1998	0	4.8	399.3	0	4.8	398.8
22-09-2001	0	25.5	192.3	0	25	192.4
01-08-2002	0	1.2	285.8	0	1.2	285.8
20-04-2001	0	35.4	239.5	0	32.3 (9%)	242.5

4 Discrepancies and Misfits

4.1 Computational complexity

The results obtained in the simulation study of the previous section show that important performance improvements can be accomplished when HMPC is applied to sewer networks. Furthermore, the hybrid modeling methodology is very rich and allows the straightforward treatment of hybrid phenomena such as overflow and flooding.

However, the underlying optimization problem of HMPC is combinatorial and $\mathcal{NP}$-hard [40]. The worst-case computation time is exponential in the number of logical variables. Figure 14 shows how this problem appears in the case of the HMPC applied on the Barcelona sewer network case study. In the top graph, rain intensity measured by the five rain gauges available in this part of the network is presented for the critical portion (second rain peak) of the rain episode occurred on October 17, 1999. This episode was relatively intensive with a return rate of 0.7 years within the city of Barcelona. In the second graph, the computation time to solve the MIP associated with the HMPC is shown as a function of time for the same scenario. Recalling that the desired sampling time for this system is 300 seconds, it can be seen that the MIP solver is unable to find the optimum within the desired sampling time. Furthermore, it is seen that computation time varies greatly. Before sample 16 the calculation time is very small.

If optimality is not archived within a desired sampling time, feasibility is at least required. Often feasibility is sufficient for proof of stability of MPC scheme, see [35]. The ILOG CPLEX solver used in the current application can be configured to put special emphasis on finding a feasible solution before an optimal one [1]. It is also possible to limit the time the solver has to solve the problem at hand. In the second graph of Fig. 14, the time required to find a feasible solution is shown. It was found by iteratively increasing the maximum solution time allowed for the solver until a feasible solution was found. The feature of CPLEX to put emphasis on finding feasible solution was activated. Again, it can be seen that the time required to find a feasible solution varies considerably. Furthermore, it should be stated that the feasible solutions found were often of such poor quality that running the system in open loop often yielded better performance.

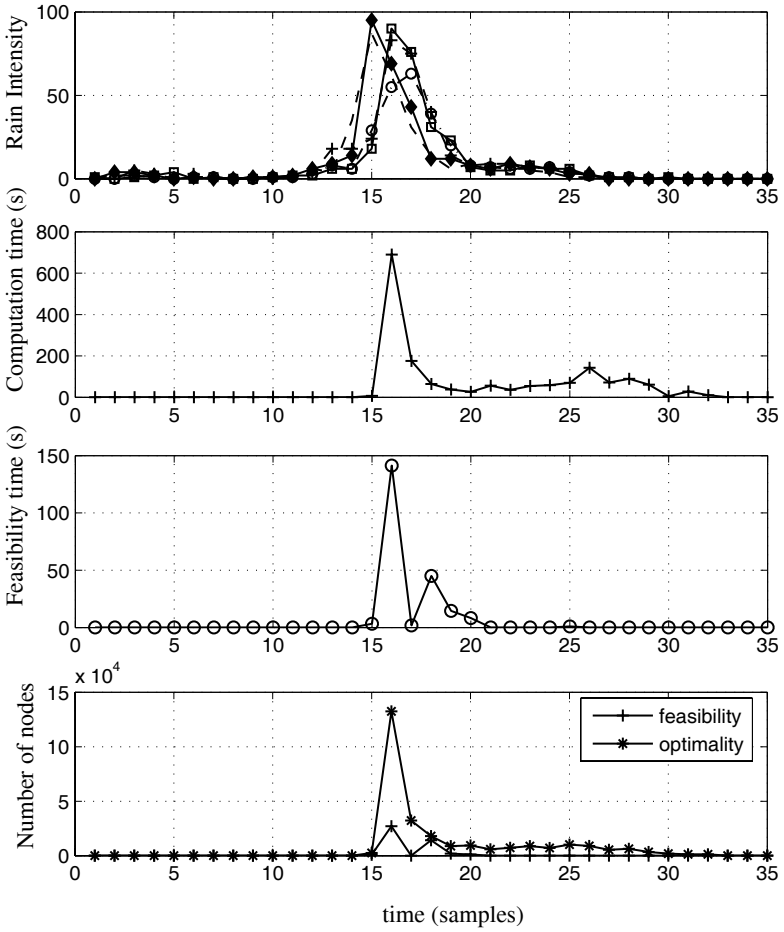

Fig. 14. MIP problem characteristics for the rain episode occurred on October 17, 1999

In the current application, the MIQP problem solved in each sample has the following generical form:

$$\min_{\rho} \quad \rho^T H \rho + f^T \rho \tag{29}$$

$$\text{s.t} \quad A\rho \leq b + Cx_0 \tag{30}$$

where vector x_0 collects the system initial conditions and predicted disturbances (rain), which is the only thing that changes from sample to sample. The ability of the MIP solver to reduce computation time from the worst-case depends on its ability to exclude from consideration as many nodes as possible when branching and bounding. This is done either by proving them to be infeasible or that their solution is suboptimal to other solutions. The increase in computation time is thus linked to an increase in the amount of feasible nodes. In the bottom graph of Fig. 14, the number of nodes the CPLEX solver explored during branching is shown. It is seen

that there was a huge increase in number of explored nodes between samples. There is thus a dramatic change in the complexity of the optimization problem for certain values of x_0.

Physical insight into the network dynamic behavior can explain the increase in complexity at time 11. At that time, due to the rain, many of the virtual tanks are very close to their overflow limit. This in turn means that more trajectories for distinct switching sequences Δ_k are feasible. Similar behavior was encountered in other rain episodes and when other cost functions were used.

The same problem regarding computation time occurs in non-linear MPC, see [32]. When the optimization problem is no longer convex, a fundamental question is how long will the optimization take and whether the quality of the solution would be sufficient to justify the application of the MPC control approach.

It should be noted that it is common engineering practice to model the hybrid dynamics of sewer systems with *max* or *min* functions and apply nonlinear MPC schemes [34]. However, the problem of finding a feasible solution is not avoided and the Non-linear Programming Algorithms applied reach only a local optima which implies a suboptimal solution. Generally heuristical methods are used to find an initial feasible solution.

4.2 Strategies to deal with the complexity in HMPC

Control strategies have been proposed where the HMPC problem is relaxed to make it computationally tractable. In [12] a *decentralized control* approach to HMPC was presented. The class of systems considered were those made up of dynamically uncoupled subsystems but where global control objectives were formulated with a global cost function.

A number of authors have also presented methods where the intent is to reduce complexity off-line. In [11] an explicit solution to the constrained finite-time optimal control problem was presented for discrete-time linear hybrid systems. *Mode enumeration* (ME) [3, 23, 24] is an off-line technique to compute and enumerate explicitly the feasible modes of piecewise affine PWA models. By pruning redundant modes where the dynamics are the same as in other modes, complexity of the hybrid model can be reduced. Such methods are usually limited to systems of relatively small size.

The main source of complexity in the MIP problem is its combinatorial nature. In [27], a HMPC strategy was presented where additional restrictions were added to the MIP problem to reduce the number of possible combinations of the Boolean variables. Infeasibility is avoided by restricting the number of combinations around a nominal feasible trajectory.

4.3 Phase transitions in MIP problems

Performance of MIP solvers has improved greatly the last years [9]. The size limit of problems considered to be practically solvable has increased steadily. Part of the reason lies in the many order of magnitudes improvement of desktop computing power over the years. But there has also been tremendous improvement in solution algorithms for LP's and QP's, which are a cornerstone of MIP solvers [8]. Furthermore, modern solvers have incorporated many performance improving features that have existed in the literature such as cutting plane capabilities. Generally the solvers apply a barrage of techniques on each problem. A recent improvement in solving the optimal control problem of HMPC by using symbolic techniques to solve constraint satisfactions problems (CSP), was presented in [6].

The MIP problem is still NP-complete and equivalent to the archetypal NP-complete K-satisfiability problem [37] (or the ZERO ONE INTEGER PROGRAMMING problem (ZIOP),

see [10]). It has recently been shown that K-satisfiability problems exhibit phase transitions in terms of computational difficulty and solution character when these aspects are considered as a function of parameters such as the ratio of number of constraints to number of variables. Away from the phase transition region the problems become easier to solve, see [37] and references therein. This is of interest as it can give information about how the problem can be modified to distance it from the phase transition region where it is most difficult to solve. *Phase transition* behavior has been reported in for example multi-vehicle task assignment problems, see [20].

4.4 Conclusions

Results presented in this chapter has shown that HMPC is a suitable control strategy for sewer networks. The hybrid modeling framework presented can take into account several inherent phenomena and elements that result in distinct behavior depending on the state of the network.

However, the exponential increase in computational complexity due to the NP-hard nature of the underlying HMPC optimization problems is a issue that should be addressed in order to face time constrains imposed by real-time implementation. For the case study presented, it has been shown that the computational complexity of the MIP problem related to the HMPC scheme can vary considerably depending on the measured state and disturbances.

Some techniques to address the computational complexity have been mentioned. Moreover, the existence of phase transitions in similar combinatorial problems should be explored to gain information on how modify the optimization problem to move it to regions of less computational complexity.

Acknowledgements

The support received by the Research Commission of the *Generalitat de Catalunya* (ref. 2005SGR00537) and the Spanish CICYT (ref. DPI2006-11944) are gratefully acknowledged. We also appreciate the support provided by CLABSA.

References

[1] (2003). *ILOG CPLEX 9.1 User´s Manual*.

[2] Ames, A. and Sastry, S. (2005). Characterization of zeno behavior in hybrid systems using homological methods. *Proceedings of the IEEE American Control Conference*, pp. 1160–1165. Portland, OR, USA.

[3] Bemporad, A. (2004). Efficient conversion of mixed logical dynamical systems into an equivalent piecewise affine form. *IEEE Trans. Automatic Control* **49**(5), 832–838.

[4] Bemporad, A. (2006). *Hybrid Toolbox - User's Guide*.

[5] Bemporad, A., Borrelli, F., and Morari, M. (2002). *Hybrid Systems: Computation and Control*, volume 228 of *Lecture Notes of Computer Science*, chapter On the optimal control law for linear discrete time hybrid systems, pp. 105–119. Springer, Berlin.

[6] Bemporad, A. and Giorgetti, N. (2006). Logic-based solution methods for optimal control of hybrid systems. *IEEE Transactions of Automatic Control* **51**(6), 963–976.

[7] Bemporad, A. and Morari, M. (1999). Control of systems integrating logic, dynamics, and constraints. *Automatica* **35**(3), 407–427.

[8] Bixby, R. (2002). Solving real-world linear programs: a decade and more of progress.
[9] Bixby, R., Fenelon, M., Gu, Z., Rothberg, E., and Wunderling, R. (2000). Mip: Theory and practice – closing the gap .
[10] Blondel, V. and Tsitsiklis, J. (2000). A survey of computational complexity results in systems and control. *Automatica* **36**, 1249–1274.
[11] Borrelli, F., Baotić, M., Bemporad, A., and Morari, M. (2005). Dynamic programming for constrained optimal control of discrete-time linear hybrid systems. *Automatica* **41**, 1709–1721.
[12] Borrelli, F., Keviczky, T., Balas, G., Stewart, G., Fregene, K., and Godbole, D. (2005). *Hybrid Decentralized Control of Large Scale Systems*, volume 3414, chapter p. 168, pp. 168–183. Springer Berlin / Heidelberg.
[13] Branicky, M. and Zhang, G. (2000). Solving hybrid control problems: Level sets and behavioral programming. *Proceedings of the IEEE American Control Conference*.
[14] Branicky, M. S., Borkar, V. S., and Mitter, S. K. (1998). A unified framework for hybrid control: Model and optimal control theory. *IEEE Transactions on Automatic Control* **43**(1), 31–45.
[15] Camacho, E. and Bordons, C. (2004). *Model Predictive Control*. Springer-Verlag, London, second edition.
[16] Cembrano, G. and Quevedo, J. (1999). *Optimization in water networks*. Research Studies Press.
[17] Cembrano, G., Quevedo, J., Salamero, M., Puig, V., Figueras, J., and Martí, J. (2004). Optimal control of urban drainage systems: a case study. *Control Engineering Practice* **12**(1), 1–9.
[18] CLABSA, C. d. B. S. (2005). Homepage. http://www.clabsa.es/.
[19] Duchesne, S., Mailhot, A., Dequidt, E., and Villeneuve, J. (2001). Mathematical modeling of sewers under surcharge for real time control of combined sewer overflows. *Urban Water* **3**, 241–252.
[20] Earl, M. and D'Andrea, R. (2005). Phase transitions in the multi-vehicle task assignment problem. *Proceedings of IMECE2005 2005 ASME International Mechanical Engineering Congress and Exposition*.
[21] Ermolin, Y. (1999). Mathematical modelling for optimized control of Moscow's sewer network. *Applied Mathematical Modelling* **23**, 543–556.
[22] Gelormino, M. and Ricker, N. (1994). Model-predictive control of a combined sewer system. *International Journal of Control* **59**, 793–816.
[23] Geyer, T. (2005). *Low Complexity Model Predictive Control in Power Electronics and Power Systems*. Ph.D. thesis.
[24] Geyer, T., Torrisi, F., and Morari, M. (2003). Efficient Mode Enumeration of Compositional Hybrid Models. *Hybrid Systems: Computation and Control* **2623**, 216–232.
[25] Heemels, W., De Schutter, B., and Bemporad, A. (2001). Equivalence of hybrid dynamical models. *Automatica* **37**, 1085–1091.
[26] Heymann, M., Lin, F., Meyer, G., and Resmerita, S. (2002). *Analysis of Zeno Behaviors in Hybrid Systems*. Technical report, Technion - Computer Science Department.
[27] Ingimundarson, A., Ocampo-Martinez, C., and Bemporad, A. (2007). Suboptimal model predictive control of hybrid systems using mode sequence constraints. Submmited to CDC 2007.
[28] Lazar, M., Heemels, W., Weiland, S., and Bemporad, A. (2006). Stability of hybrid model predictive control. *IEEE Transactions of Automatic Control* **51**(11), 1813 – 1818.
[29] Lincoln, B. and Rantzer, A. (2001). Optimizing linear system switching. *Proceedings of the 40th IEEE conference on Decision and Control*, pp. 2063–2068.

[30] Ljung, L. (1999). *System Identification—Theory for the User, Second Edition*. Prentice Hall.

[31] Lygeros, J., Tomlin, C., and Sastry, S. (1999). Controllers for reachability specifications for hybrid systems. *Automatica* **35**(3), 349 – 370.

[32] Maciejowski, J. (2002). *Predictive Control with Constraints*. Prentice Hall, Great Britain.

[33] Marinaki, M. and Papageorgiou, M. (1998). Nonlinear optimal flow control for sewer networks. *Proceedings of the IEEE American Control Conference*, volume 2, pp. 1289–1293.

[34] Marinaki, M. and Papageorgiou, M. (2005). *Optimal Real-time Control of Sewer Networks*. Springer.

[35] Mayne, D., Rawlings, J., Rao, C., and Scokaert, P. (2000). Constrained model predictive control: Stability and optimality. *Automatica* **36**, 789–814.

[36] Mays, L. (2004). *Urban Stormwater Management Tools*. McGrawHill.

[37] Monasson, R., Zecchina, R., Kirkpatrick, S., Selman, B., and Troyansky, L. (1999). Determining computational complexity from characteristic "phase transitions". *Nature* **400**, 133–137.

[38] Ocampo-Martinez, C., Puig, V., Quevedo, J., and Ingimundarson, A. (2005). Fault tolerant model predictive control applied on the Barcelona sewer network. *Proceedings of IEEE Conference on Decision and Control (CDC) and European Control Conference (ECC)*.

[39] Ocampo-Martínez, C., Ingimundarson, A., Puig, V., and Quevedo, J. (2007). Objective prioritization using lexicographic minimizers for MPC of sewer networks. *IEEE Transactions on Control Systems Technology* (Accepted for publication).

[40] Papadimitriou, C. (1994). *Computational Complexity*. Addison-Wesley.

[41] Pleau, M., Colas, H., Lavallée, P., Pelletier, G., and Bonin, R. (2005). Global optimal real-time control of the Quebec urban drainage system. *Environmental Modelling & Software* **20**, 401–413.

[42] Pleau, M., Methot, F., Lebrun, A., and Colas, A. (1996). Minimizing combined sewer overflow in real-time control applications. *Water Quality Research Journal of Canada* **31**(4), 775 – 786.

[43] Schilling, W., Anderson, B., Nyberg, U., Aspegren, H., Rauch, W., and Harremöes, P. (1996). Real-time control of wasterwater systems. *Journal of Hydraulic Resourses* **34**(6), 785–797.

[44] Schütze, M., Butler, D., and Beck, B. (2002). *Modelling, Simulation and Control of Urban Wastewater Systems*. Springer.

[45] Schütze, M., Campisanob, A., Colas, H., W.Schillingd, and Vanrolleghem, P. (2004). Real time control of urban wastewater systems: Where do we stand today? *Journal of Hydrology* **299**, 335–348.

[46] Schütze, M., To, T., Jaumar, U., and Butler, D. (2002). Multi-objective control of urban wastewater systems. *Proceedings of 15th IFAC World Congress*.

[47] Schutter, B. D. (1999). Optimal control of a class of linear hybrid systems with saturation. *Proceedings of 38th IEEE Conference on Decision and Control*, pp. 3978–3983.

[48] Singh, V. (1988). *Hydrologic systems: Rainfall-runoff modeling*, volume I. Prentice-Hall, N.J.

[49] Smith, K. and Austin, G. (2000). Nowcasting precipitation - A proposal for a way forward. *Journal of Hydrology* **239**, 34–45.

[50] Tomlin, C., Lygeros, J., and Sastry, S. (2000). A game theoretic approach to controller design for hybrid systems. *Proceedings of the IEEE*, volume 88, pp. 949–970.

[51] Torrisi, F. and Bemporad, A. (2004). Hysdel - A tool for generating computational hybrid models for analysis and synthesis problems. *IEEE Trans. Contr. Syst. Technol.* **12**(2), 235–249.

[52] Weyand, M. (2002). Real-time control in combined sewer systems in Germany: Some case studies. *Urban Water* **4**, 347 – 354.

[53] Yuan, J., Tilford, K., Jiang, H., and Cluckie, I. (1999). Real-time urban drainage system modelling using weather radar rainfall data. *Phys. Chem. Earth (B)* **24**, 915–919.